LETTER

Design of a fully differential current mode operational amplifier with improved input–output impedances and its filter applications

Mustafa Altun*, Hakan Kuntman

Faculty of Electrical and Electronics Engineering, Department of Electronics and Communication Engineering, Istanbul Technical University, 34469 Maslak, Istanbul, Turkey

Abstract

In this paper, a CMOS implementation of a fully differential current-mode operational amplifier (COA) is presented. To achieve very low input resistance, a new technique based on a positive feedback is used in the input transimpedance stage. Additionally, traditional current output stage (Arbel Goldminz output stage) with improved output resistance is selected as a transconductance stage. Results of simulations exhibit 96 dB DC gain, nearly 120 Ω input, 30 MΩ output resistances and a gain-bandwidth product exceeding 90 MHz. The proposed COA is operated under ±1.5 V voltage supplies and designed with 0.35-μm CMOS process. Furthermore, COA-based fourth-order band-pass (BP) filter consisting of Butterworth low-pass (LP) and high-pass (HP) filters is realized as an application example. SPICE simulation results are included to verify correctness of the designs.
© 2007 Elsevier GmbH. All rights reserved.

Keywords: Fully differential COA; COA-based filters

1. Introduction

In recent years, current-mode approach has been extensively investigated. Compared to the voltage-mode circuits, current mode circuits have some significant advantages such as inherent wide bandwidth, wide dynamic range and simple circuitry with lover voltage supplies [1,2]. Current-mode operational amplifier (COA) is one of the useful current-mode integrated building blocks. The main advantage of using COA is its ability to replace with the voltage operational amplifier (VOA) when applying the adjoint network theorem in voltage mode to current mode transformation [3].

The circuit symbol of fully differential COA is reported in Fig. 1. COA ideally exhibits zero input resistance and infinite output resistance and current gain.

It is not difficult to increase output resistance and current gain to reasonable values. On the other hand, to get very low input resistance, some complicated negative feedback configurations have been suggested [4,5] and it generally worsens frequency response of the amplifier. Moreover, these structures cause bigger problems in fully differential COA's because of its double input. Positive feedback is another solution for getting better input resistance [6,7]. This paper presents a new approach dependent on positive feedback to decrease input resistance.

Traditional current output stage (Arbel Goldminz output stage) is the most commonly used transconductance stage but it suffers from its output resistance [8]. A novel current output stage with Improved output resistance is proposed in this study.

In the literature, most of the COA designs are single-ended. However, fully differential analog signal processing provides several advantages over single-ended analog signal

---
* Corresponding author. Tel.: +90 212 285 6419; fax: +90 212 285 35 65.
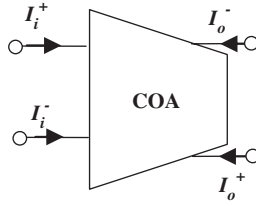*E-mail address:* altunmus@itu.edu.tr (M. Altun).

Fig. 1. Circuit symbol of fully differential COA.

processing. Some CMOS implementations of fully differential COA have been reported [9–11]. Unfortunately, these COA's do not offer low input resistance and most of them do not have proper frequency response. The proposed fully differential COA has simple circuitry and offers high performance.

Some useful current amplifier based filter applications have been presented in the literature [12,13]. To demonstrate the performance of the proposed COA, a new fourth-order band-pass (BP) filter that enables maximal flatness around the center frequency is proposed.

2. Proposed COA

As shown in Fig. 2, the proposed amplifier has very simple structure. W/L of transistors and DC values of the circuit are reported in Tables 1 and 2, respectively.

The amplifier is configured from a differential input transimpedace stage followed by a differential output transconductance stage. Shown in dashed lines at the input stage,

M2, M4 and M10, M11 compose positive feedback loops to reduce positive and negative input resistances, respectively. Because, only four more transistors are used for input resistance improvements, frequency response of the amplifier is not noteworthy affected by these additional transistors.

Eqs. (1) and (2) show input resistances without positive feedback loops and generally their values are not low enough.

$$r_{\text{in}-} \cong \frac{1}{g_{m1}}, \tag{1}$$

$$r_{\text{in}+} \cong \frac{1}{g_{m9}}. \tag{2}$$

Input resistance equations of the proposed COA are shown in (3) and (4). The second terms of (3) and (4) mainly affect input resistance value. If we select its value close to zero, r_{in} also goes near zero. Moreover, its value must bigger than zero to overcome the stability problem. If we choose $g_{m3} = g_{m4}$, $g_{m1} = g_{m2}$ and $g_{m11} = g_{m12}$, $g_{m9} = g_{m10}$, then we will both overcome stability problem and obtain very low input resistances. Consequently we come such a decision that $(W/L)_{\text{M3}} = (W/L)_{\text{M4}}$, $(W/L)_{\text{M1}} = (W/L)_{\text{M2}}$, $(W/L)_{\text{M11}} = (W/L)_{\text{M12}}$, $(W/L)_{\text{M9}} = (W/L)_{\text{M10}}$. Furthermore, because positive feedback is increasing stability problem, MOS transistor matching parameters are also considered in this study. To analyze the MOS transistor mismatches, firstly we need to calculate variances of relative currentgain factor (K) mismatch—$\sigma(\Delta K/K)$—and threshold voltage (VT) mismatch—$\sigma(\Delta VT)$—for transistors M1–M4 and M9–M12. As it will be reported in the

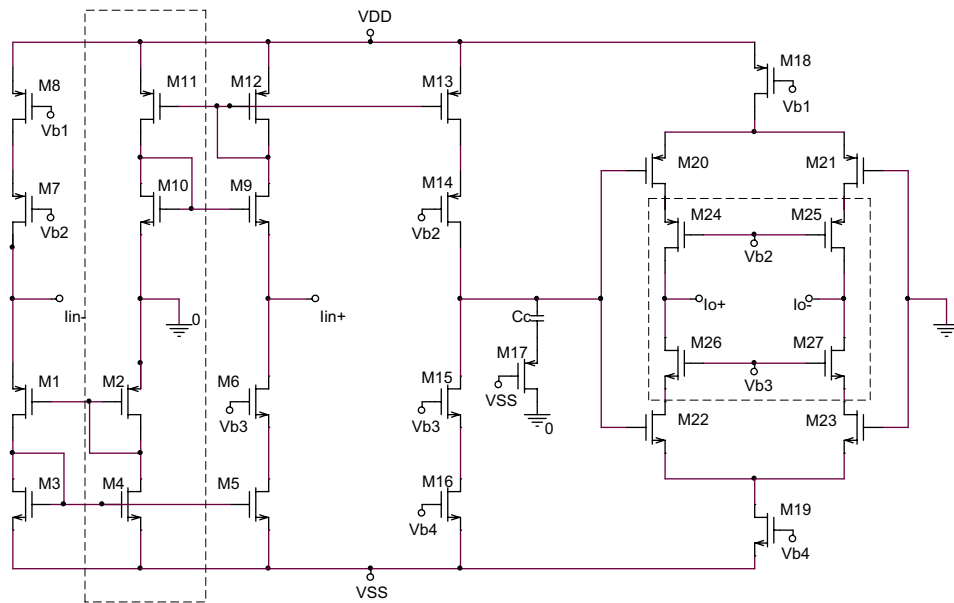**Fig. 2.** Schematic of the proposed COA.

Table 1. Transistor dimensions

Transistors	$W(\mu m)/L(\mu m)$
M1, M2	20/0.7
M3, M4, M5, M6	20/1
M7	10/0.7
M8	27/0.7
M9, M10	15/0.7
M11, M12, M13	20/1.4
M14	40/1.4
M15	20/0.7
M16	17.8/1.4
M17	12.5/1
M18	118/1
M19	47/1
M20, M21	75/1
M22, M23	40/0.7
M24, M25	100/1
M26, M27	60/0.7

Table 2. DC values of the COA

Parameter	Value
$V_{DD} - V_{SS}$	$\pm 1.5\,V$
V_{b1}, V_{b2}	$0.6\,V, -0.3\,V$
V_{b3}, V_{b4}	$0.3\,V, -0.8\,V$
I_{D8}, I_{D16}	$30\,\mu A$
I_{D18}, I_{D19}	$100\,\mu A$

'Simulation Results' part, input resistances stay positive while considering the matching parameters in worst case.

$$r_{in-} \cong \frac{1}{g_{m1}g_{m3}}\left[(g_{ds1} + g_{m3} + g_{ds3})\right.$$
$$\left. - \frac{g_{m1}g_{m4}}{g_{ds4} + g_{m2} + g_{ds2}}\right], \qquad (3)$$

$$r_{in+} \cong \frac{1}{g_{m9}g_{m12}}\left[(g_{ds9} + g_{m12} + g_{ds12})\right.$$
$$\left. - \frac{g_{m9}g_{m11}}{g_{ds11} + g_{m10} + g_{ds10}}\right]. \qquad (4)$$

Output resistance of traditional current output stage (Arbel Goldminz output stage) is shown in Eq. (5).

$$r_{out+} = r_{out-} \cong \left[\left(\frac{g_{m20}g_{ds21}}{g_{m21} + g_{m20}}\right) + \left(\frac{g_{m22}g_{ds23}}{g_{m23} + g_{m22}}\right)\right]^{-1}. \quad (5)$$

M24, M25, M26 and M27 in dashed line are added to the conventional current output stage for getting very big output resistance values. The output resistance equation of the proposed COA is represented in (6). Compared to the conventional one, proposed output stage approximately offers $g_m r_o$ times higher output resistance.

$$r_{out+} = r_{out-} \cong \left[\left(\frac{g_{m20}g_{ds21}g_{ds25}}{g_{m25}(g_{m21} + g_{m20})}\right)\right.$$
$$\left. + \left(\frac{g_{m22}g_{ds23}g_{ds27}}{g_{m27}(g_{m23} + g_{m22})}\right)\right]^{-1}. \qquad (6)$$

Transistor M17 operates like a resistance (Rc) and improves frequency response of the COA. Cc is inserted at the high impedance node for compensation. DC current gain and gain-bandwidth product are given by (7) and (8), respectively.

$$A_i(0) \cong \frac{g_{m20}g_{m22}}{2}\left[\frac{g_{ds14}g_{ds13}}{g_{m14}} + \frac{g_{ds15}g_{ds16}}{g_{m15}}\right]^{-1}, \qquad (7)$$

$$f_{GBW} \cong \frac{1}{2\pi}\frac{g_{m20} + g_{m22}}{2Cc}. \qquad (8)$$

3. COA-based filter realizations

The proposed second-order low-pass (LP) and high-pass (HP) filter configurations are shown in Fig. 3. Single COA is used for each realization and matching conditions are
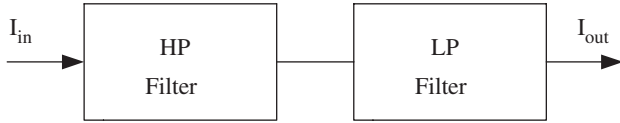
$R_1 = R_3 = R_{LP}, C_1 = C_2 = C_{LP}$ for LP filter,
$R_4 = R_5 = R_{HP}, C_4 = C_6 = C_{HP}$ for HP filter.

The node analysis of the circuit of Fig. 3(a) yields current transfer function as follows:

$$\frac{i_{out-LP}}{i_{in}} = \frac{\dfrac{1}{2R_{LP}R_2C_{LP}^2}}{s^2 + s\dfrac{1}{R_2C_{LP}} + \dfrac{1}{2R_{LP}R_2C_{LP}^2}}. \qquad (9)$$
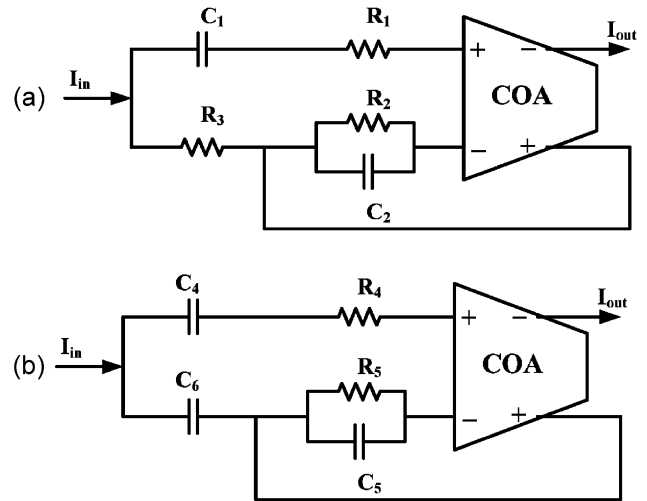
Fig. 3. (a) COA-based low-pass filter topology; (b) COA-based high-pass filter topology.

Fig. 4. Band-pass filter structure formed by high-pass and low-pass filters.

The natural angular frequency w_0 and the quality factor Q of the LP filter can be expressed as

$$w_0 = \sqrt{\frac{1}{2R_{LP}R_2C_{LP}^2}}, \quad Q = \sqrt{\frac{R_2}{2R_{LP}}}. \tag{10}$$

It should be noted that w_0 and Q are orthogonally adjustable. It means that w_0 can be adjusted without disturbing the Q by changing either C_{LP} or R_{LP} and R_2 simultaneously while R_2/R_{LP} is constant. Sensitivity analysis of the LP filter shows that

$$S_{R_{LP}}^{w_0} = S_{R_2}^{w_0} = -1/2, \; S_{C_{LP}}^{w_0} = -1, \; S_{R_2}^{Q} = 1/2, \; S_{R_{LP}}^{Q} = -1/2,$$

which are equal-less than unity in magnitude.

The node analysis of the circuit of Fig. 3(b) yields current transfer function as follows:

$$\frac{i_{out-HP}}{i_{in}} = \frac{s^2}{s^2 + s\dfrac{1}{R_{HP}C_{HP}} + \dfrac{2}{R_{HP}^2 C_{HP}C_5}}. \tag{11}$$

The natural angular frequency w_0 and the quality factor Q of the HP filter can be expressed as

$$w_0 = \sqrt{\frac{2}{R_{HP}^2 C_{HP}C_5}}, \quad Q = \sqrt{\frac{C_{HP}}{2C_5}}. \tag{12}$$

It should be again noted that w_0 and Q are orthogonally adjustable. It means that w_0 can be adjusted without disturbing the Q by changing either R_{HP} or C_{HP} and C_5 simultaneously while C_{HP}/C_5 is constant. Sensitivity analysis of the HP filter shows that

$$S_{C_{HP}}^{w_0} = S_{C_5}^{w_0} = -1/2, \; S_{R_{HP}}^{w_0} = -1, \; S_{C_{HP}}^{Q} = 1/2, \; S_{C_5}^{Q} = -1/2,$$

which are equal-less than unity in magnitude.

As shown in Fig. 4, it is possible to realize BP filter by using HP and LP filters connecting one's output to another's input. With using this BP filter structure, we can arrange the passband width.

4. Simulation results

4.1. Simulation results of the proposed COA

SPICE is used for simulation with the process parameters of a 0.35 μm CMOS technology. BSIM3v3 parameter sets

Table 3. Performance parameters of the COA

Parameter	Value
Power dissipation	0.66 mW
Open-loop gain	96 dB
GBW	92 MHz
Phase margin (Cc = 1.2 p Rc = 2.4 kΩ)	60°
Output voltage range	±0.6 V
Slew rate	4 μA/ns
Input resistance (n)	124 Ω
Input resistance (p)	109 Ω
Output resistance	30 MΩ
Input voltage offset (n)	≈ 1.6 mV
Input voltage offset (p)	≈ −3.5 mV

are used for modelling transistors of which threshold voltages are nearly 0.5 V for NMOS and −0.7 V for PMOS. The transistor widths range from 5 to 120 μm.

Table 3 summarizes the performance of the COA. The COA provides 96 dB DC gain, 92 MHz UGBW and 60° phase margin guaranteeing single pole behaviour throughout the UGBW. Input and output resistance values are also fairly good. For transistors M1–M4 and M9–M12, $\sigma(\Delta VT)$ values are calculated between 2.1 and 3.9 mV and $\sigma(\Delta K/K)$ values are calculated between 0.16% and 0.27%. As a result, input resistances become +52 Ω (n) and +47 Ω (p) for the worst case (still positive). Because of the class A operation, speed of the COA is limited by quiescent current. Open loop frequency characteristic is seen from Fig. 5. The transient response to a step input current of ±5μA is shown in Fig. 6.

Note that if we did not use impedance improvements, input resistance and output resistance values would be nearly 2.5 and 340 kΩ, respectively. On the other hand, output voltage range would be better, nearly ±0.9 V.

4.2. Simulation results of the COA-based filter

Shown in Fig. 4, BP filter configuration is simulated by choosing the passive element values of LP filter C_{LP}=7.5 pF, $R_{LP} = R_2 = 5$ kΩ which results in a natural frequency of $f_0 \approx 3.0$ MHz and a quality factor of $Q = 0.707$ and for BP filter $C_{HP} = C_5 = 15$ pF, $R_{HP} = 50$ kΩ which results in a natural frequency of $f_0 \approx 300.1$ kHz and a quality factor of $Q = 0.707$. So that, center frequency of the BP filter is 1 MHz and this configuration enables maximally flat passband.

From Fig. 7 it can be understood that the theoretical and simulation results are in good agreement. The dependence of the output harmonic distortion of BP filter on input current amplitude is illustrated in Fig. 8 . From Fig. 8, we can see that the harmonic distortion rapidly increases if the input signal is increased beyond 180 μA for the chosen fully differential COA implementation.
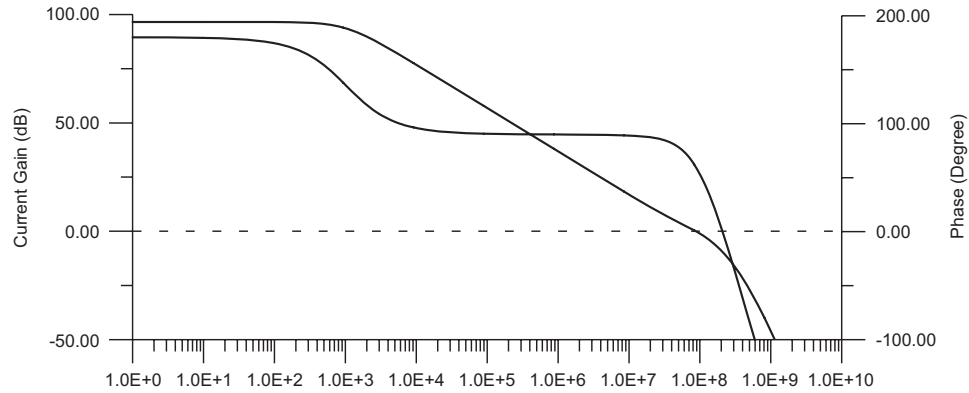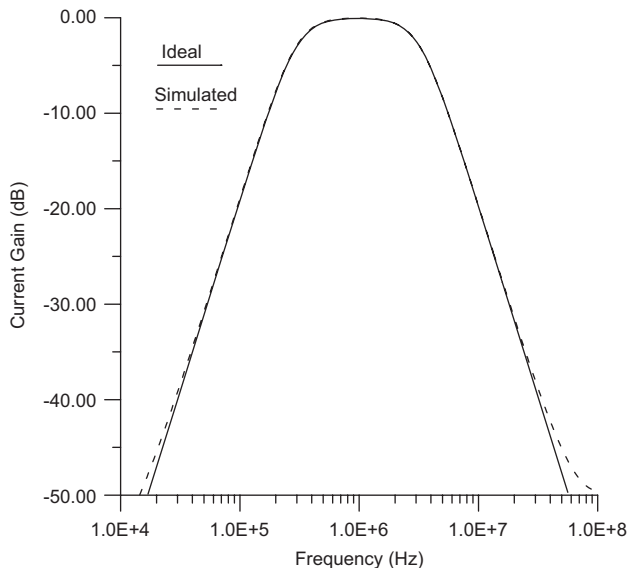
Fig. 5. Open-loop frequency response of the COA.
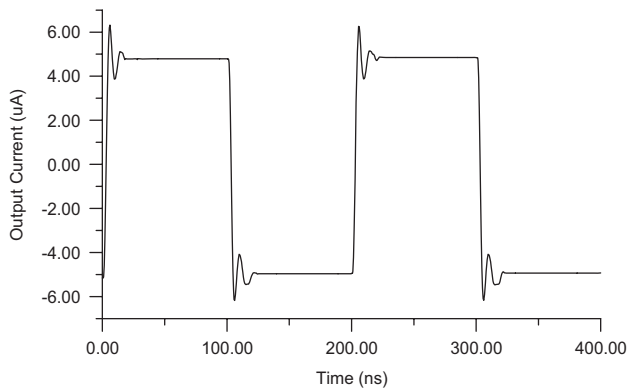
Fig. 6. Response of the COA in unity-gain feedback to a $\pm 5\,\mu$A input step ($f = 5$ MHz).
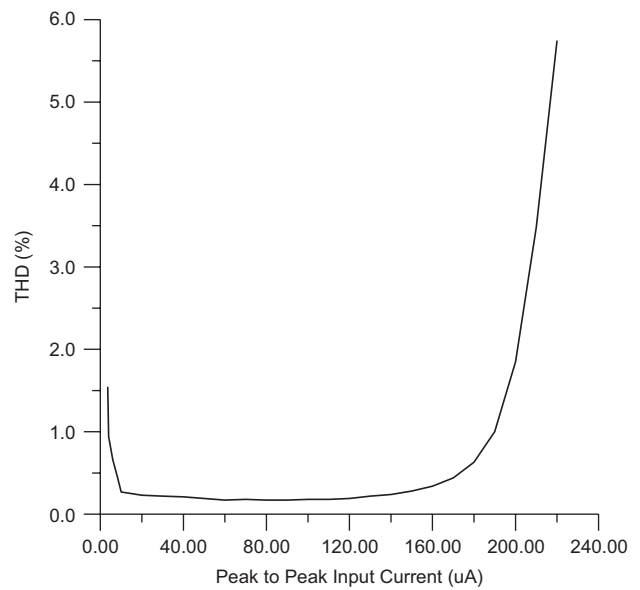
Fig. 8. Total harmonic distortion (THD) values of the filter versus input peak to peak current at 1 MHz frequency.

5. Conclusion

In this work, very accurate, fully differential COA is proposed and simulation results are presented. A novel approach is used in input resistance improvement and also very high output resistance is achieved by modifying traditional current output stage. Due to the simple circuitry of the proposed COA, higher than 90 MHz GBW is obtained. It also offers very high DC gain and ± 0.6 V output voltage swing. As an application example, a new COA-based fourth-order BP filter is proposed. Simulation results of the filter are the evidences of accuracy of the proposed fully differential COA.

References

[1] Palmisano G, Palumbo G, Pennisi S. CMOS current amplifiers. Boston, MA: Kluwer Academic Publishers; 1999.

Fig. 7. Simulated and ideal band-pass filter responses.

[2] Toumazou C, Lidgey FJ, Haigh DG. Analog IC design: the current-mode approach. London: Peter Peregrinus Ltd.; 1990.

[3] Roberts GW, Sedra AS. A general class of current amplifier-based biquadratic. filter circuits. IEEE Trans Circuits Syst 1992;39:257–63.

[4] Surakampontorn W, Riewruja V, Kumwachara K, Dejhan K. Accurate CMOS-based current conveyors. IEEE Trans Instrum Meas 1992;40:699–702.

[5] Palmisano G, Palumbo G. A simple CMOS CCII+. Int J Circuit Theory Appl 1995;23(6):599–603.

[6] Wang W. Wideband class AB (push–pull) current amplifier in CMOS technology. Electron Lett 1990;26(8):543–5.

[7] Altun M, Kuntman H. A wideband CMOS current-mode operational amplifier and its use for band-pass filter realization. In: Proceedings of applied electronics, Pilsen, 2006, p. 3–6.

[8] Arbel AF, Goldminz L. Output stage for current-mode feedback amplifiers, theory and applications. Analog Integrated Circuits Signal Process 1992;2:243–55.

[9] Cheng KH, Wang HC. Design of current mode operational amplifier with differential input and differential output. In: Proceedings of IEEE international symposium on circuits and systems, Hong Kong, 1997, p. 153–156.

[10] Jun S, Kim DM. Fully differential current operational amplifier. Electron Lett 1998;34:62–3.

[11] Kaulberg T. A CMOS current-mode operational amplifier. IEEE J Solid-State Circuits 1993;28(7):849–52.

[12] Souliotis G, Chrisanthopoulos A, Haritantis L. Current differential amplifiers: new circuits and applications. Int J Circuit Theory Appl 2001;29(6):553–74.

[13] Kilinc S, Cam U. Current-mode first-order allpass filter employing single current operational amplifier. J Analog Integrated Circuits Signal Process 2004;41:47–53.